Title

Inhibition of MRTF activation as a clinically achievable anti-fibrotic mechanism for pirfenidone.

Permalink

Journal

Authors

Ma, Hsiao-Yen
Vander Heiden, Jason
Uttarwar, Salil
et al.

Publication Date

DOI

Copyright Information

Peer reviewed

Inhibition of MRTF activation as a clinically achievable anti-fibrotic mechanism for pirfenidone

Hsiao-Yen Ma[1], Jason A. Vander Heiden [2], Salil Uttarwar[2], Ying Xi [1,3], Elsa-Noah N'Diaye[1,4], Ryan LaCanna[1], Patrick Caplazi [5,6], Sarah Gierke[5], John Moffat[7], Paul J. Wolters[8] and Ning Ding [1]

[1]Department of Discovery Immunology, Genentech, South San Francisco, CA, USA. [2]Department of OMNI Bioinformatics, Genentech, South San Francisco, CA, USA. [3]School of Life Science and Technology, ShanghaiTech University, Shanghai, China. [4]Gilead Sciences, Foster City, CA, USA. [5]Department of Pathology, Genentech, South San Francisco, CA, USA. [6]AbbVie, South San Francisco, CA, USA. [7]Department of Biochemical and Cellular Pharmacology, Genentech, South San Francisco, CA, USA. [8]Department of Medicine, University of California, San Francisco, CA, USA.

Corresponding author: Ning Ding (ding.ning@gene.com)

Abstract

Background Idiopathic pulmonary fibrosis (IPF) is a progressive fibrotic disease characterised by aberrant fibroblast/myofibroblast accumulation and excessive collagen matrix deposition in the alveolar areas of lungs. As the first approved IPF medication, pirfenidone (PFD) significantly decelerates lung function decline while its underlying anti-fibrotic mechanism remains elusive.

Methods We performed transcriptomic and immunofluorescence analyses of primary human IPF tissues.

Results We showed that myocardin-related transcription factor (MRTF) signalling is activated in myofibroblasts accumulated in IPF lungs. Furthermore, we showed that PFD inhibits MRTF activation in primary human lung fibroblasts at clinically achievable concentrations (half-maximal inhibitory concentration 50–150 µM, maximal inhibition >90%, maximal concentration of PFD in patients <100 µM). Mechanistically, PFD appears to exert its inhibitory effects by promoting the interaction between MRTF and actin indirectly. Finally, PFD-treated IPF lungs exhibit significantly less MRTF activation in fibroblast foci areas than naïve IPF lungs.

Conclusions Our results suggest MRTF signalling as a direct target for PFD and implicate that some of the anti-fibrotic effects of PFD may be due to MRTF inhibition in lung fibroblasts.

Introduction

Idiopathic pulmonary fibrosis (IPF) is a progressive and fatal interstitial lung disease with a median survival of 3–5 years after diagnosis [1–4]. Although the underlying pathobiology of IPF is complex and poorly understood, it is proposed that the disease is likely triggered by repetitive microinjuries to the airway and alveolar epithelium [5]. These parenchymal insults lead to the activation and accumulation of myofibroblasts in interstitial areas of lungs. Consequently, these myofibroblasts synthesise and deposit excessive amounts of extracellular matrix proteins into alveolar regions, which results in progressive lung function decline and, ultimately, patient death [6, 7]. Therefore, IPF represents a huge unmet medical need for the global public health system [5–8].

Numerous experimental therapies have failed in clinical trials of IPF and, to date, only two medications have been approved for the treatment of IPF patients, pirfenidone (PFD) and nintedanib (NTD), based on their ability to slow disease progression as measured by reduced lung function decline [9, 10]. While NTD has been proposed to target fibroblast and myofibroblast proliferation and activation as a potent multiple receptor tyrosine kinase inhibitor [11, 12], the anti-fibrotic mechanism of PFD remains elusive. In this regard, it should be noted that recent studies have linked PFD to a wide spectrum of biological activities

such as targeting pro-fibrotic growth factors and transcription factors, inhibiting collagen fibril formation, and antagonising oxidative stress [13–18]. However, the limitation of these studies is the use of excessive concentrations of PFD and/or the lack of human evidence. Thus, the clinical relevance of these observations has not been fully established and the molecular target(s) for PFD in patients are yet to be defined [19, 20].

Serum response factor (SRF) is an important transcription factor that regulates cytoskeleton and cell motility gene expression *via* the interaction with its two main coactivators: myocardin-related transcription factor A and B (MRTFA/B) [21–26]. In unstimulated cells, MRTFA is largely sequestered in cytoplasm by binding to monomeric actin (G-actin) *via* its N-terminal arginine-proline-glutamate-leucine consensus sequence-containing (RPEL) domain [23, 27–29]. When cells are stimulated, Ras homologue (Rho) GTPases are activated to trigger polymerisation of G-actin to filamentous actin (F-actin), thereby releasing MRTFs from G-actin and allowing them to be predominantly translocated into the nucleus to induce cytoskeleton gene expression *via* interaction with SRF [23, 27–29]. The critical role of MRTF signalling in cell motility and cytoskeleton reprogramming is further supported by human genetics data that MRTFA loss-of-function mutation causes immune susceptibility to viral infections and aberrant wound healing response due to compromised motility of immune cells and fibroblasts [17]. Mouse studies have also demonstrated that MRTF signalling contributes to tissue fibrosis in multiple pre-clinical models [30–36].

Here, we hypothesise that certain dysregulated molecular pathway(s) in human IPF lungs may be targeted by PFD for its anti-fibrotic action. Using transcriptomic analyses of human samples, we found that MRTF signalling is induced in human IPF lungs and its hyperactivation appears to be specific to mesenchymal cells, including fibroblasts and myofibroblasts. Furthermore, the complementary immunofluorescence analysis revealed that MRTF activation appears to be mainly derived from α-smooth muscle actin (ACTA2)-expressing myofibroblasts accumulated in IPF lungs. Next, we showed that PFD inhibits MRTFA nuclear translocation, a central cellular event of MRTF signalling activation, and MRTF target gene expression in a dose-dependent manner. The potency of PFD on antagonising MRTF signalling was further experimentally determined as half-maximal inhibitory concentration (IC_{50}) 50–150 µM and maximal inhibition >90%. Mechanistically, we observed that PFD promotes the interaction between MRTF and actin indirectly without impacting Rho family member A (RhoA) activation and actin polymerisation. Consistent with these findings, PFD-treated but not NTD-treated IPF lungs exhibit less MRTF activation in fibroblast foci than those in naïve IPF lungs without PFD treatment. In sum, these data suggest MRTF signalling as a direct molecular pathway that can be inhibited by PFD at physiologically relevant concentrations, which may represent a new and clinically achievable anti-fibrotic mechanism for the drug.

Materials and methods

Patient cohort

All human sample acquisitions were approved by the University of California at San Francisco (UCSF) (San Francisco, CA, USA) Institutional Review Board. The clinical profile and demographic information of IPF patients and healthy control subjects is provided in supplementary table S1. The IPF patient cohort treated with or without PFD or NTD has been reported previously [37]. In this cohort, the mean duration of PFD treatment was 22.7 months (range 9–60 months) and the mean duration of NTD treatment was 13.4 months (range 7–20 months) [37].

Human lung samples

Explanted lung tissues were obtained from patients with a pathological diagnosis of usual interstitial pneumonia and a consensus clinical diagnosis of IPF assigned by multidisciplinary discussion and review of clinical materials. Written informed consent was obtained from all subjects and the study was approved by the UCSF Institutional Review Board. Human lungs not used by the Northern California Transplant Donor Network were used as controls; studies indicate that these lungs are physiologically and pathologically normal [38]. After perfusion of the pulmonary arteries and bronchoalveolar lavage, fresh lung explant tissue was stored in complete media on wet ice overnight before subsequent digestion. IPF lung biopsies treated with or without PFD or NTD were described previously [37].

Primary human lung cell isolation

The tissue was washed in Hanks' buffered salt solution (HBSS) and then thoroughly minced in digestion buffer (HBSS, 2.5 mg·mL^{-1} collagenase D and 100 µg·mL^{-1} DNase). Minced tissue was rocked for 45 min at 37°C. Residual tissue material was transferred into fresh digestion buffer and rocked for another 45 min at 37°C. Single cells from both rounds of digest were combined and then filtered through 70- and 40-µm strainers. Red blood cells were removed using Red Blood Cell Lysis Buffer (Sigma-Aldrich, St Louis, MO, USA). The cell preparations were stained with anti-human CD45-BUV395 (1:250; BD

Biosciences, Franklin Lakes, NJ, USA), anti-human EPCAM-PE (1:250; BioLegend, San Diego, CA, USA), anti-human CD31 PerCP-Cy5.5 (1:250; BioLegend) and Fixable Viability Dye eFluor 780 (1:2000; Thermo Fisher Scientific, Waltham, MA, USA), and sorted by fluorescence-activated cell sorting for EPCAM$^+$, CD31$^+$, CD45$^+$ and triple-negative populations using BD FACSAria and analysed with FlowJo.

Cell culture

A539, U937, MLE12, HL60 and THP1 cells were purchased from ATCC (Manassas, VA, USA). Primary human lung artery endothelial cells were purchased from ScienCell (Carlsbad, CA, USA). These primary cells were cultured as instructed by the vendors. Primary human lung fibroblasts were isolated from crude whole-lung single-cell suspension and cultured in DMEM supplemented with 2 mM L-glutamine, 100 U·mL^{-1} penicillin, 100 µg·mL^{-1} streptomycin and 10% fetal bovine serum (FBS). U937 cells were differentiated into macrophage-like cells by 20 ng·mL^{-1} phorbol-12-myristate-13-acetate (PMA) (Cayman Chemical, Ann Arbor, MI, USA) treatment for 24 h prior to serum-free medium (SFM) starvation and FBS stimulation. HL60 cells were differentiated into neutrophil-like cells by 1.5% (v/v) dimethyl sulfoxide treatment for 6 days prior to SFM starvation and FBS stimulation. THP1 cells were differentiated into dendritic cell-like cells by 20 ng·mL^{-1} interleukin-4 (R&D Systems, Minneapolis, MN, USA) and 20 ng·mL^{-1} PMA for 4 days prior to SFM starvation and FBS stimulation.

RNA sequencing

RNA from lung fibroblasts was extracted using the RNeasy Kit (Qiagen, Hilden, Germany) and treated with DNase I (Life Technologies, Carlsbad, CA, USA). The libraries were generated with the TruSeq Stranded mRNA Kit (Illumina, San Diego, CA, USA) and were sequenced on the HiSeq system 2500 in high output mode.

RNA sequencing analysis

Sequencing reads for both lung data published herein and previously published liver data (European Nucleotide Archive accession ERP109255) were filtered and aligned using HTSeqGenie v3.4.1 [39]. GSNAP v2011-12-28 was used for alignment, through the HTSeqGenie wrapper, against the GENCODE Basic gene model on the human genome assembly GRCh38. Only reads with unique genomic alignments were analysed.

Normalised reads per kilobase gene model per million total reads (nRPKM) values were used as a normalised measure of gene expression, calculated as previously defined [40]. $\log_2$ nRPKM transformations were calculated on nRPKM+1^{-4} and the z-scored $\log_2$ nRPKM ranges displayed in the heatmaps were restricted to ±3SD of the $\log_2$ nRPKM values for visualisation purposes; heatmap clustering was performing using Ward's method. Differential gene expression was calculated using voom+limma [41] with multiple-hypothesis correction of p-values performed using the Benjamini–Hochberg method. Significance tests of the MRTF response gene set compared with background were performed using the parametric camera method on the log fold change distributions [42].

For differential gene expression and Gene Ontology (GO) analysis, upregulated genes were defined as genes having an nRPKM fold change >0 and adjusted p-value <0.05. GO analysis was performed using the Molecular Signatures Database (MSigDB) gene sets [43]. The MRTF response signature was derived from the overlap between previously reported MRTF direct target genes [24] and cytoskeleton or motility-related genes upregulated in IPF lungs. $\log_2$ nRPKM fold change distributions include all MRTF response genes against all other genes (background), excluding genes which did not have at least 10 reads in at least 10% of the samples. Sample signature scores for the MRTF response gene set were defined as the first principal component score of a principal component analysis calculated on the $\log_2$ nRPKM of the MRTF response gene set (eigengene). All RNA sequencing (RNA-seq) analyses were conducted in R [44].

Immunofluorescence staining

Sections (4 µm) of formalin-fixed and paraffin-embedded specimens were deparaffinated followed by antigen retrieval using Target Retrieval (Dako, Glostrup, Denmark). The sections were subsequently blocked and stained in PBS plus 1% bovine serum albumin (Gibco, Carlsbad, CA, USA), 5% nonimmune donkey serum (Jackson ImmunoResearch, West Grove, PA, USA) and 0.1% Triton X-100. The following primary antibodies were used for immunofluorescence: anti-MRTFA (1:100; Sigma-Aldrich), anti-ACTA2-FITC (1:250; Sigma-Aldrich), anti-EPCAM (1:500; Cell Signaling Technology, Danvers, MA, USA), anti-CD45 (1:400; Cell Signaling Technology) and anti-CD31 (1:1000; Cell Signaling Technology). Human sections were imaged with a 20× Plan Apo DIC M objective (NA: 0.75) on a Nikon Ti-Eclipse (Nikon, Tokyo, Japan) inverted microscope equipped with an Andor Neo scMOS camera (Oxford Instruments, Abingdon, UK), a linear-encoded automated stage (Applied Scientific

Instrumentation, Eugene, OR, USA) and a SOLA LED light engine (Lumencor, Beaverton, OR, USA) all run by NIS Elements software (Nikon).

Transfection of small interfering RNAs

Transfection was carried out at a concentration 20 nM of indicated small interfering RNAs (Horizon Discovery, Cambridge, UK) using RNAiMax transfection reagent (Thermo Fisher Scientific). Transfected cells were cultured without perturbation for at least 48 h prior to SFM starvation and 20% FBS stimulation.

Reverse transcriptase quantitative PCR

Cultured primary human normal and IPF lung fibroblasts were starved with SFM overnight and then treated with 20% FBS and PFD or NTD at the indicated concentrations for another 24 h. Subsequently, cells were harvested for RNA extraction. Total RNA was purified using the RNeasy Kit (Qiagen) and treated with DNase I (Life Technologies). Complementary DNA synthesis was carried out with iScript RT Supermix (Bio-Rad, Hercules, CA, USA). Quantitative PCR was performed in technical triplicates using SYBR Green reagent (Bio-Rad). The relative standard curve method was used for quantitation and expression levels were calculated by normalisation to hypoxanthine phosphoribosyltransferase.

Western blot

Western blot was carried out on whole-cell extracts or nuclear extracts as described previously [45]. Equal amounts of protein lysates were separated by SDS–PAGE, transferred to a nitrocellulose membrane and subjected to immunoblotting analysis using the following primary antibodies: MRTFA (1:200; Santa Cruz Biotechnology, Dallas, TX, USA), YY1 (1:1000; Abcam), GAPDH (1:1000; Cell Signaling Technology) and ACTB (1:200; Santa Cruz Biotechnology).

Cell-based functional assays

For the proliferation assay, primary human lung fibroblasts cultured in 96-well plates were treated with PFD at the indicated concentrations for 48 h followed by CellTiter-Glo assay (Promega, Madison, WI, USA). For the RhoA activation assay, primary human lung fibroblasts were starved in SFM for 24 h, then treated with 20% FBS plus PFD at the indicated concentrations for 2 h and intracellular RhoA activity was measured using the RhoA G-LISA Activation Assay Kit (Cytoskeleton, Denver, CO, USA). For the F-actin formation assay, primary human lung fibroblasts starved in SFM for 24 h were treated with 20% FBS plus PFD (1 mM) or Latrunculin B (LanB) (100 nM) for 2 h followed by fixation in 4% paraformaldehyde, permeabilisation in 0.1% saponin and staining with 0.33 µM rhodamine phalloidin solution in a sequential order. Cells were then thoroughly washed and bound phalloidin was extracted by 30 min incubation with pure methanol. F-actin content was determined by measuring rhodamine phalloidin fluorescence using 537 nm for excitation and 576 nm for emission.

Pulldown assays

For pulldown assays using cell extracts, Ni-NTA agarose (Thermo Fisher Scientific) was saturated with 6×His peptides or His-RPEL fusion protein from *Escherichia coli* lysates, washed and used as affinity resin, which was subsequently incubated with cytoplasmic extracts from primary human lung fibroblasts, generated by lysis in hypotonic buffer (10 mM HEPES (pH 7.9), 10 mM KCl, 1.5 mM $MgCl_2$, 0.1 mM dithiothreitol (DTT) and protease inhibitors) through syringing and removal of insoluble material by centrifugation. An equivalent of a confluent 10-cm dish of primary human lung fibroblasts was used for one binding reaction. For pulldown assays in a reconstituted system, affinity resin saturated with 6×His peptides or His-RPEL protein was incubated with purified actin protein (Cytoskeleton) instead of cytoplasmic extracts from primary human lung fibroblasts. Binding reactions in both assays were for 2 h in binding buffer (50 mM Tris–HCl (pH 7.5), 250 mM NaCl, 1 mM $MgCl_2$, 0.2 mM ATP, 0.1 mM DTT and protease inhibitors) supplemented with 0.5% Triton X-100. The resin was then washed three times in binding buffer without protease inhibitors and subjected to 4–20% SDS–PAGE. The high-molecular-weight (>25 kDa) section of the gel was used for actin Western blotting (4970; Cell Signaling Technology) and the low-molecular-weight (<25 kDa) section of the gel was Coomassie blue stained to reveal bait input.

Quantification and statistical analysis

Custom scripts in R version 3.5.1 were utilised for RNA-seq data analysis and plotting. Prism (GraphPad, La Jolla, CA, USA) was utilised for plotting and statistical analysis. Statistical details of experiments can be found in the figure legends, including the statistical tests used and value and definition of n.

Results

MRTF signature is enriched in IPF lungs

In order to advance our understanding of the pathobiology of human lung fibrosis, we performed genome-wide transcriptomic analysis on freshly explanted human lungs from patients with IPF and nondiseased controls [46]. In parallel, transcriptional profiles were also collected from mesenchymal cells isolated directly from the same lungs *via* triple-negative (CD45⁻EPCAM⁻CD31⁻) sorting (figure 1a and supplementary figure S1). GO analysis revealed that biological processes such as cell projection represented by cilium-associated genes and cell movement were among the top upregulated processes in IPF lungs, which is consistent with previous reports (figure 1b) [47–52]. In addition, cytoskeleton and its related cell motility pathways were also enriched in the upregulated genes from IPF lungs (figure 1b). We then sought to determine whether enrichment of cytoskeleton and motility genes was caused by dysregulation of gene expression in mesenchymal cells or, alternatively, by aberrant accumulation of mesenchymal cell populations such as fibroblasts/myofibroblasts in fibrotic lungs. Upon cell sorting, we found that cytoskeleton and cell motility were still among the top upregulated biological processes in sorted IPF mesenchymal cells (figure 1b), suggesting enrichment of these processes is likely due to transcriptional changes rather than imbalances in cellularity.

To identify underlying transcriptional conduits responsible for cytoskeleton and motility gene expression, we explored potential transcription factors that may contribute to cytoskeleton and motility reprogramming by using MSigDB [53], and found that SRF putative target genes are highly enriched in cytoskeleton and motility genes upregulated in IPF lungs among top hits (figure 1c). As SRF stimulates motility and cytoskeleton gene expression *via* MRTFs [21–26], we next aimed to determine if MRTF signalling is hyperactive in fibrotic lungs by generating a MRTF response signature to measure its activity. The distribution of relative expression for the MRTF response signature (IPF *versus* nondiseased lungs) displayed a marked shift compared with that of all other genes analysed (figure 1d). Unsupervised clustering analysis of nondiseased controls and IPF patients using the same MRTF signature showed a separation between nonfibrotic and fibrotic samples (figure 1e and f). We also performed a similar analysis of the MRTF signature in another previously reported IPF cohort [54]. Consistently, we found a significant enrichment of the MRTF signature in IPF lungs when compared with healthy controls (supplementary figure S2a–c). Thus, the observations from two independent IPF cohorts support the hyperactivation of MRTF signalling in IPF lungs.

MRTF activation in myofibroblasts in IPF lungs

To investigate the cellular source of MRTF activation, we performed immunofluorescence assays to examine MRTFA nuclear localisation, a molecular hallmark of MRTF activation, in IPF lungs. In this regard, we observed a prominent MRTFA nuclear localisation in ACTA2⁺ myofibroblasts accumulated in the fibroblast foci, a histological feature of IPF lungs (figure 2a and e). It should also be noted that diffuse MRTFA signal was observed in both cytoplasm and nuclei in EPCAM⁺ epithelial cells (figure 2b and e), implicating less MRTF activation in these cells than that in myofibroblasts. On the other hand, we only found negligible cytoplasmic and nuclear MRTFA signal in CD31⁺ endothelial cells and CD45⁺ immune cells (figure 2c–e). Therefore, these results suggest that myofibroblasts may be the main cell type that mediates MRTF activation in IPF lungs.

PFD inhibits MRTF activation in a clinically relevant dose range in lung fibroblasts

The hyperactivation of MRTF signalling in IPF lung mesenchymal cells, particularly (myo)fibroblasts, prompts us to speculate that PFD may target this pathway to achieve, at least, some of its anti-fibrotic actions. Therefore, to test this possibility, we examined whether PFD could inhibit serum-induced MRTFA nuclear translocation in two independent primary human lung fibroblast lines isolated from normal and IPF human lungs, respectively. As expected, PFD attenuated serum-induced MRTFA nuclear translocation in a dose-dependent manner without compromising the overall MRTFA protein level (figure 3a and c). In addition, we did not observe any significant impact of PFD on fibrillar collagen gene expression and lung fibroblast viability (supplementary figures S2 and S3) and, consistently, a recent report suggested that MRTF signalling is not required for these two processes in fibroblasts [55]. The IC$_{50}$ for PFD on MRTF nuclear translocation is ∼100 and ∼150 µM for each fibroblast line, with the maximal inhibition reaching >90% (figure 3b, d and e). Notably, the IC$_{50}$ of PFD to inhibit MRTFA nuclear translocation is in the range of its clinically observed concentrations (<100 µM) [56–58], suggesting that partial inhibition of MRTF signalling may be achievable for PFD in human IPF patients. We also determined the impact of PFD on MRTF activation in nonfibroblastic cells such as alveolar epithelial cells, immune cells (*e.g.* neutrophils, macrophages and dendritic cells) and lung artery endothelial cells. The data showed that PFD exhibits little effect on serum-induced MRTF activation in those cell types even at the concentration of
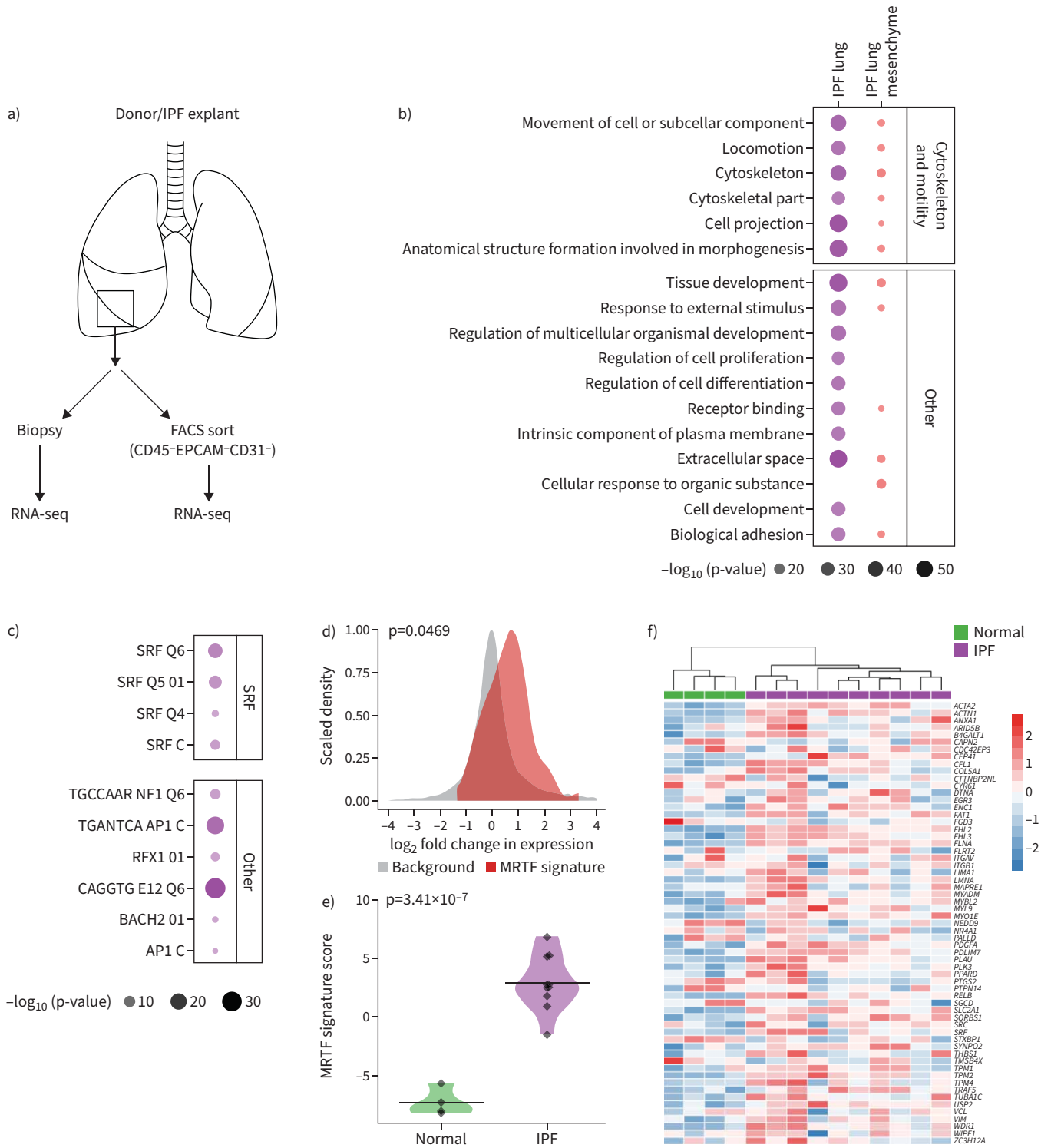
FIGURE 1 The myocardin-related transcription factor (MRTF) signature is enriched in idiopathic pulmonary fibrosis (IPF) lungs. a) Schematic overview of human sample collection. b) Top Gene Ontology biological processes enriched in genes upregulated in fibrotic samples. c) Top 10 *cis*-regulatory motifs enriched in the promoter regions of upregulated cytoskeleton and cell motility genes in IPF lungs. d) Density fit of $\log_2$ fold change distributions of IPF *versus* normal lungs. Separate distributions are shown for MRTF response genes (MRTF signature) and all other genes with expression levels passing quality control (background). The displayed density fit is truncated at the bounds of the observed $\log_2$ fold change values within each category of genes. MRTF signature≠background. e) Violin plot of the MRTF signature in normal (n=4) and IPF lungs (n=10). f) Unsupervised hierarchical clustering analysis of MRTF signature gene expression in IPF (n=10) and normal lungs (n=4). FACS: fluorescence-activated cell sorting; RNA-seq: RNA sequencing; SRF: serum response factor. p-value calculated using the unpaired two-tailed t-test.
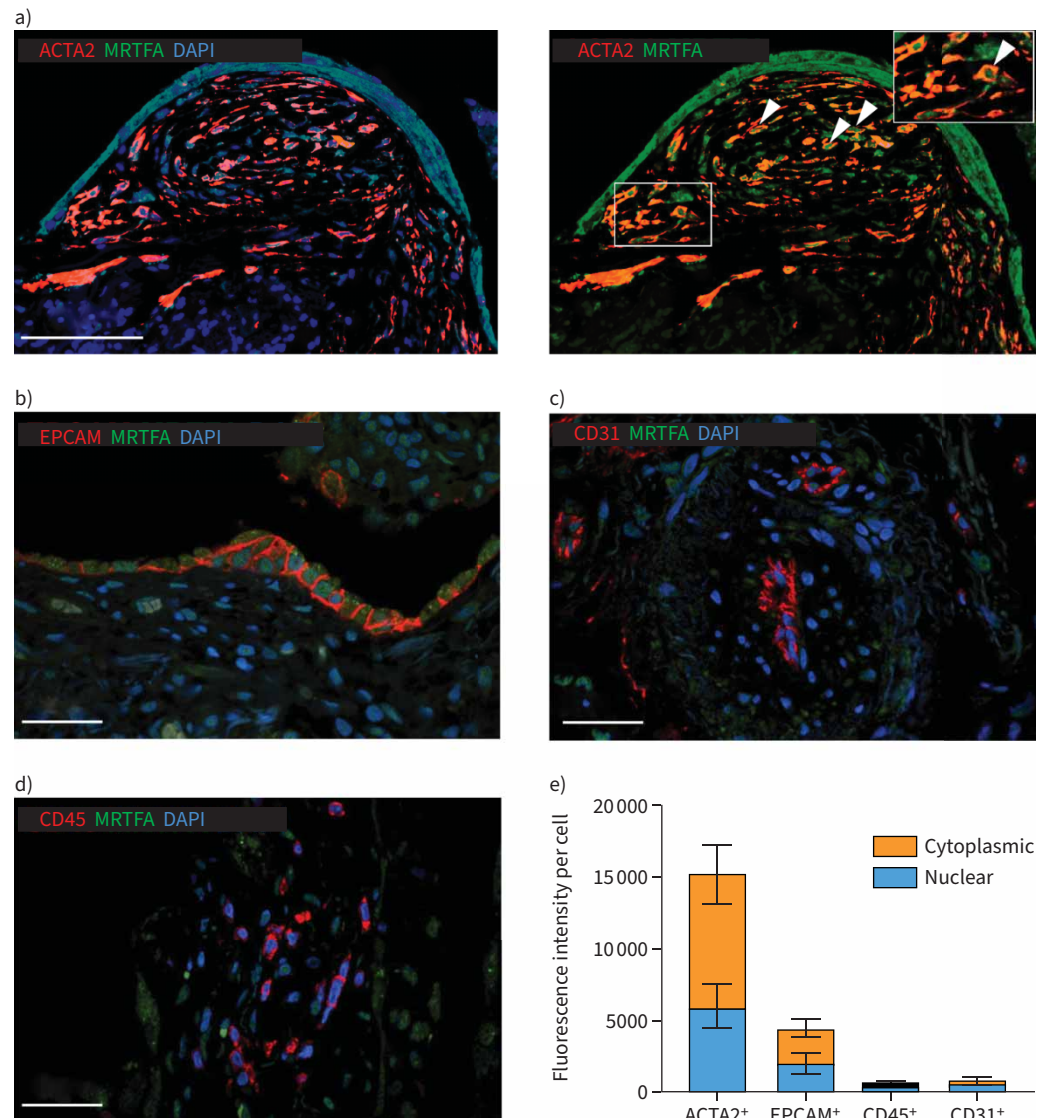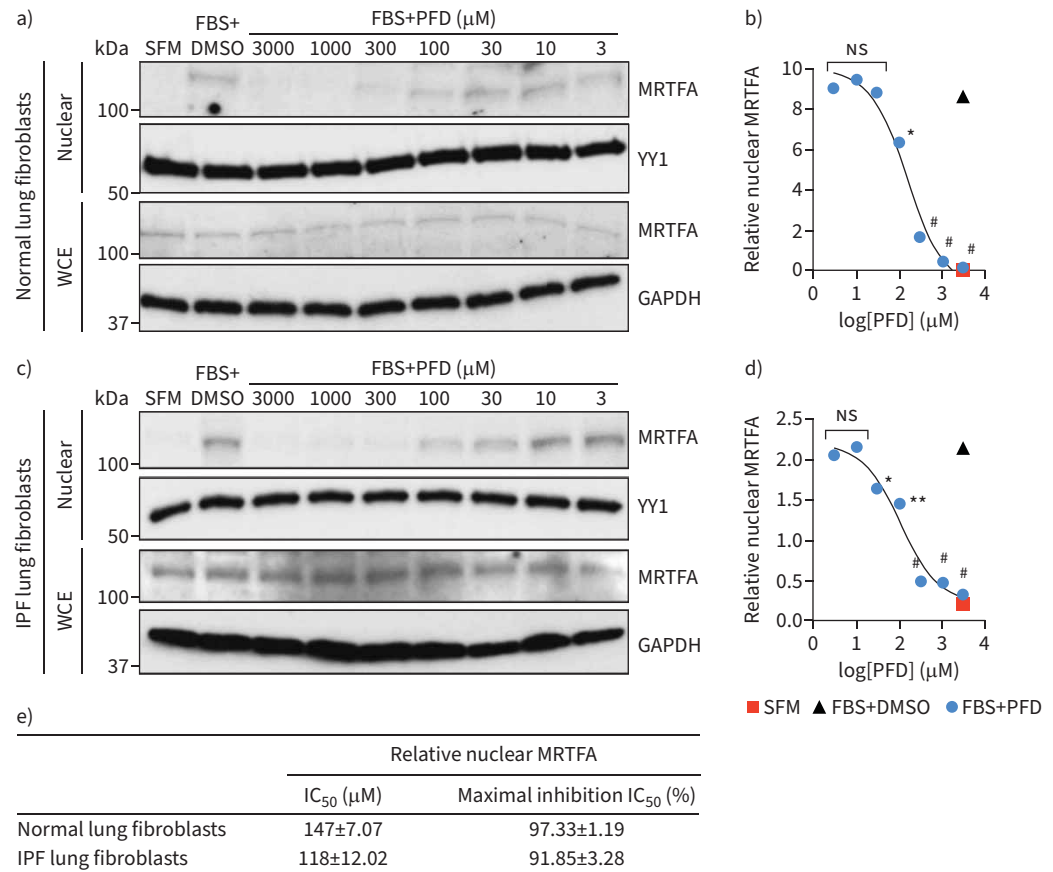
FIGURE 2 Activation of myocardin-related transcription factor (MRTF) signalling in myofibroblasts of idiopathic pulmonary fibrosis (IPF) lungs. a–d) Representative immunofluorescence images of MRTFA co-stained with a) α-smooth muscle actin (ACTA2), b) EPCAM, c) CD31 and d) CD45 in IPF lung sections. Arrowhead: nuclear MRTFA in ACTA2$^+$ myofibroblasts. Scale bar: a) 50 µm; b–d) 20 µm. e) Quantification of nuclear and cytoplasmic MRTFA fluorescent signal normalised by cell numbers in ACTA2$^+$, EPCAM$^+$, CD45$^+$ and CD31$^+$ cells in IPF lungs. IPF samples (n=10) were used for MRTFA signal quantification in EPCAM$^+$, CD45$^+$ and CD31$^+$ cells, and IPF samples (n=8) were used for MRTFA signal in ACTA2$^+$ cells due to the lack of fibroblast foci in two IPF samples. Data represent mean±SD. DAPI: 4′,6-diamidino-2-phenylindole.

1 mM (supplementary figure S4), indicating that PFD may selectively inhibit MRTF signalling in lung fibroblasts.

Transcriptomic analysis of the inhibitory effects of PFD on MRTF signalling in lung fibroblasts

Next, we sought to evaluate the systemic impact of PFD on the transcriptional response of serum-induced MRTF signalling in lung fibroblasts. We chose 1 mM PFD for this experiment as this is the concentration that PFD can achieve ⩾90% MRTF inhibition in both lung fibroblast lines tested. RNA-seq analysis of serum-stimulated primary human lung fibroblasts revealed that PFD suppressed a series of MRTF direct target genes (figure 4a and supplementary figure S5a). Consistently, GO analysis of PFD downregulated genes showed a significant functional enrichment for MRTF-related categories, including cell adhesion, cell motility, migration and cell morphogenesis (figure 4b and supplementary figure S5b).

FIGURE 3 Pirfenidone (PFD) inhibits serum-induced myocardin-related transcription factor A (MRTFA) nuclear accumulation in human lung fibroblasts at clinically relevant concentrations. a, c) Representative Western blots of nuclear (top panel) and whole-cell extract (WCE) (bottom panel) MRTFA in human a) normal and c) idiopathic pulmonary fibrosis (IPF) lung fibroblasts treated with 20% fetal bovine serum (FBS) in the absence or presence of PFD at the indicated concentrations. Ying Yang 1 (YY1) loading control for nuclear fractions. Glyceraldehyde-3-phosphate dehydrogenase (GAPDH) loading control for WCE. b, d) Quantification of nuclear accumulation of MRTFA in b) normal and c) IPF lung fibroblasts. e) Summary of PFD potency on nuclear MRTFA accumulation. Data in e) represent mean±SD of three independent experiments. SFM: serum-free media; IC$_{50}$: half-maximal inhibitory concentration. p-value calculated as FBS *versus* FBS+PFD using one-way ANOVA. *: $p < 0.05$; **: $p < 0.01$; #: $p < 0.0001$; NS: not significant.

In addition to activating MRTF signalling, serum can strongly stimulate other pathways such as ternary complex factor (TCF) [59] and Hippo signalling [60]. So, if PFD selectively targeted MRTF signalling, we would expect no significant impact of PFD on TCF or Hippo downstream target gene expression. To this end, we compared the expression of several well-established TCF and Hippo target genes stimulated by serum in the absence or presence of PFD. As expected, we observed no significant effects of PFD on the expression of those genes (figure 4a, d and e and supplementary figure S5a). Furthermore, PFD appears to suppress serum-induced MRTF target gene (*e.g.* ACTA2 and MYL9) expression through MRTFA as depletion of MRTFA completely abolishes PFD's antagonistic effects (figure 4f–h), supporting the specificity of PFD as an MRTF inhibitor.

To further investigate if these findings are clinically relevant, we determined the PFD dose–response curves of two MRTF target genes: ACTA2 and MYL9. In agreement with its inhibitory activity on MRTFA nuclear translocation (figure 3e), PFD exhibits similar potency on suppression of serum-induced ACTA2 and MYL9 expression: IC$_{50}$ ranges between 50 and 150 μM and the maximal inhibition is >90% (figure 5a–c). Taken together, these results suggest that PFD is a selective inhibitor of MRTF signalling in lung fibroblasts, at least, *in vitro*.
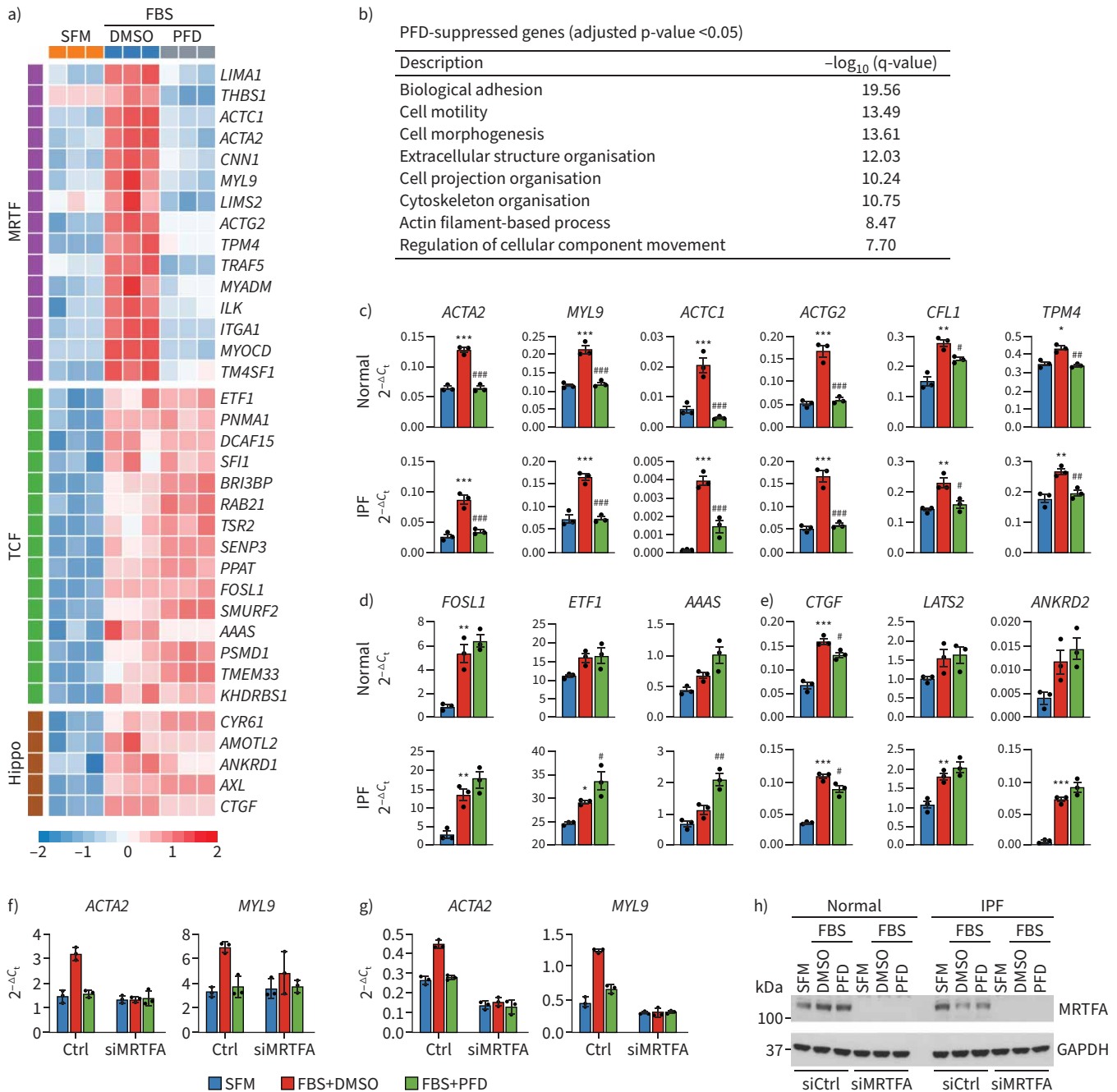
FIGURE 4 Transcriptomic analysis of pirfenidone (PFD) inhibitory effects on myocardin-related transcription factor (MRTF) signalling. a) Heatmap showing relative expression of MRTF, ternary complex factor (TCF) and Hippo target genes in normal human lung fibroblasts treated with or without PFD. b) Top Gene Ontology biological processes enriched in the genes suppressed by PFD in 20% fetal bovine serum (FBS)-stimulated normal human lung fibroblasts. c–e) Quantitative PCR validation of PFD inhibition on c) MRTF, d) TCF and e) Hippo target gene expression in normal and IPF human lung fibroblasts. f, g) *ACTA2* and *MYL9* expression in serum-free medium (SFM) or 20% FBS-stimulated f) normal and g) idiopathic pulmonary fibrosis (IPF) human lung fibroblasts transfected with MRTFA or control (Ctrl) small interfering RNA (siRNA) in the presence or absence of PFD. h) Representative Western blot of MRTFA in whole-cell extract from SFM or 20% FBS-stimulated human normal and IPF lung fibroblasts transfected with MRTFA or control siRNA in the presence or absence of PFD. Glyceraldehyde-3-phosphate dehydrogenase (GAPDH) loading control for whole-cell extract. PFD concentration: 1 mM, n=3 biological replicates. p-value calculated using one-way ANOVA. *: $p<0.05$; **: $p<0.01$; ***: $p<0.001$ indicates comparison of SFM *versus* FBS. #: $p<0.05$; ##: $p<0.01$; ###: $p<0.001$ indicates comparison of FBS *versus* FBS+PFD.
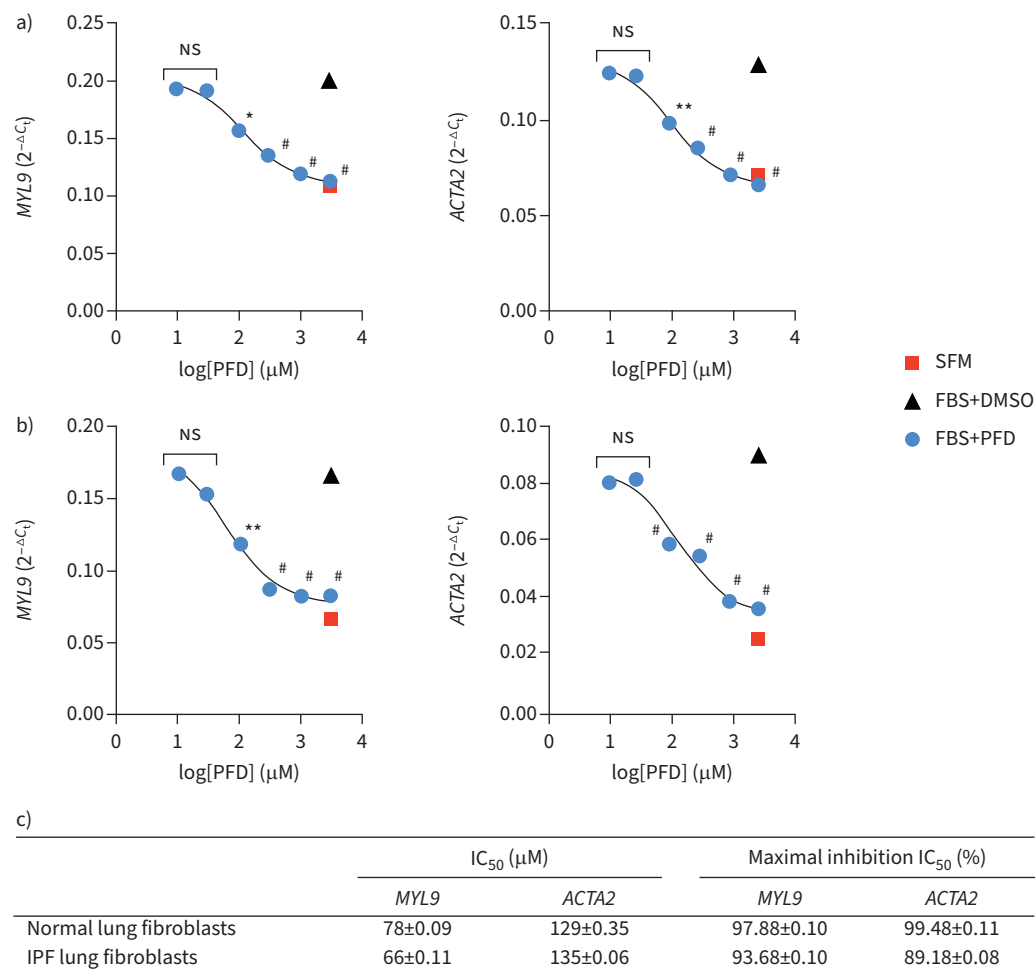
FIGURE 5 Determination of pirfenidone (PFD) inhibitory potency on myocardin-related transcription factor (MRTF) target gene expression in human lung fibroblasts. a, b) Dose–response curves of PFD inhibition on MRTF target gene expression in human a) normal and b) idiopathic pulmonary fibrosis (IPF) lung fibroblasts. c) Summary of PFD inhibitory potency on MRTF target gene expression. Data in c) represent mean±SD of three independent experiments, n=3 biological replicates. IC$_{50}$: half-maximal inhibitory concentration. p-value calculated as fetal bovine serum (FBS) *versus* FBS+PFD using one-way ANOVA. *: $p < 0.05$. **: $p < 0.01$; #: $p < 0.0001$; NS: not significant.

PFD promotes the binding of MRTF to actin indirectly

As we observed the inhibitory effects of PFD on MRTF signalling, an intriguing question arises: what could be the mechanistic bases underlying its activity against MRTF? In this regard, we considered the following three key upstream cellular events of MRTF nuclear translocation that may be affected by PFD: 1) Rho GTPase/RhoA activation, 2) actin polymerisation and 3) MRTF–actin interaction.

First, we explored whether PFD inhibits serum-induced RhoA activation and we observed no significant impact of 1 mM PFD in RhoA activation (figure 6a). Similarly, we found 1 mM PFD does not affect G-actin polymerisation into F-actin induced by serum, whereas LanB, a well-documented actin polymerisation inhibitor, can dramatically disrupt this process (figure 6b). Finally, we tested the possibility that PFD may modulate the physical interaction between MRTF and actin. We fused the actin binding domain of MRTFA, RPEL domain (2–261), with 6×His-tag (His-RPEL) and performed pulldown assays by incubating this recombinant fusion protein with the cytoplasmic extract from lung fibroblasts treated with or without PFD at the indicated concentrations. The results showed that PFD increases the recruitment of endogenous actin to His-RPEL recombinant protein in a dose-dependent manner (figure 6c). To determine whether PFD promotes this interaction directly, we repeated the pulldown assays in a reconstituted system consisting of recombinant His-RPEL fusion protein and purified actin protein, instead
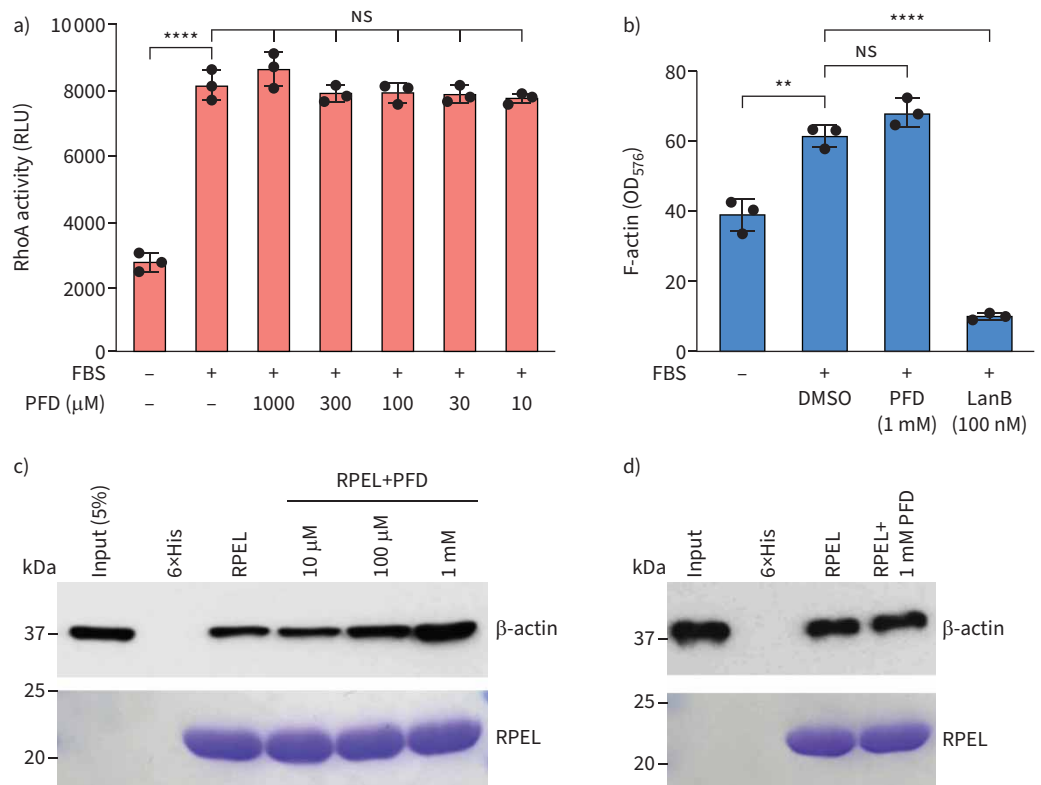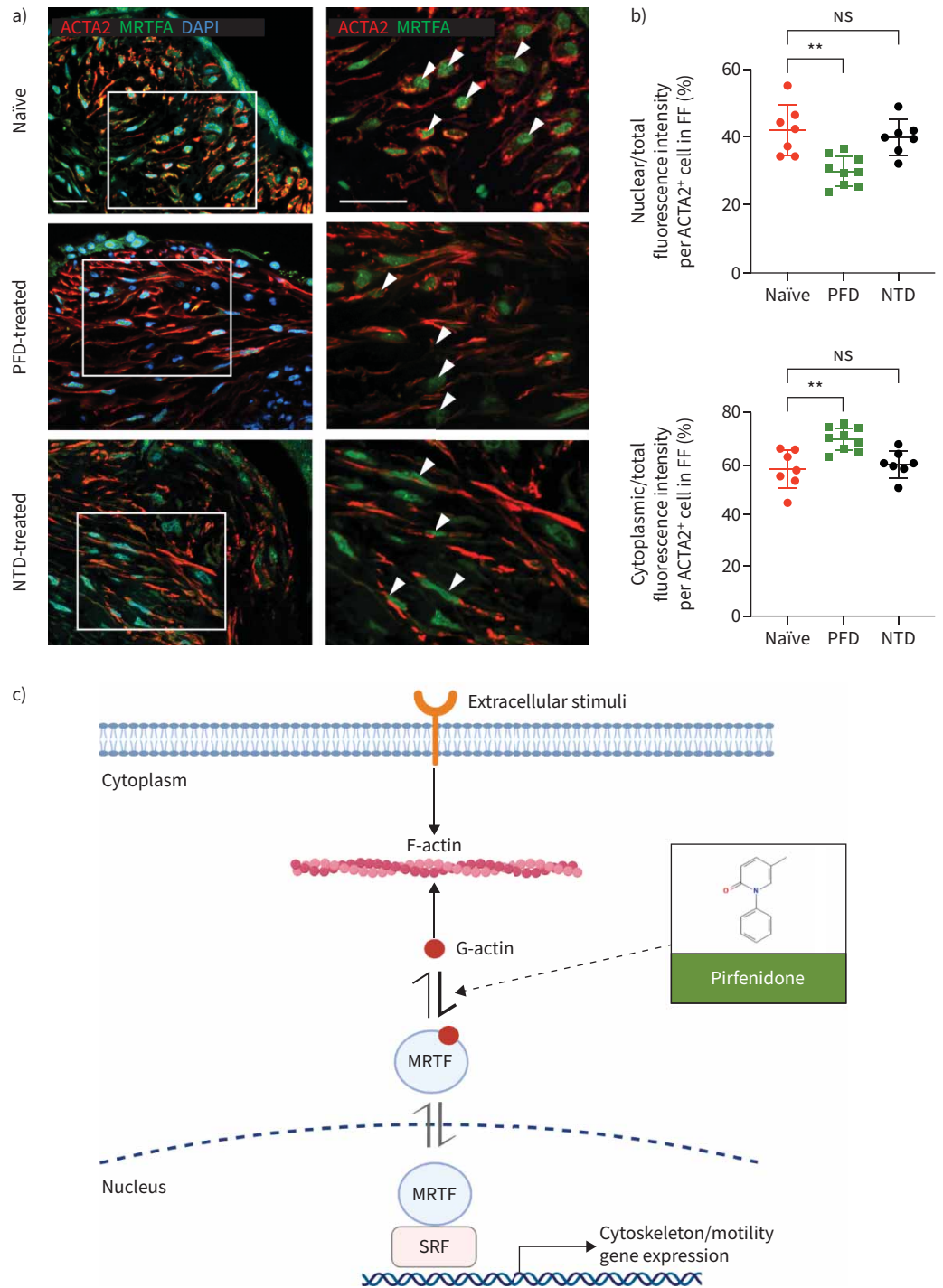
FIGURE 6 Pirfenidone (PFD) promotes myocardin-related transcription factor A (MRTFA) and actin interaction indirectly. a) Ras homologue family member A (RhoA) activation in human lung fibroblasts stimulated with 20% fetal bovine serum (FBS) in the absence or presence of PFD at the indicated concentrations. n=3 biological replicates. b) F-actin formation in human lung fibroblasts stimulated with 20% FBS in the absence or presence of 1 mM PFD or 100 nM Latrunculin B (LanB). n=3 biological replicates. c) Top panel: His-RPEL fusion protein was used to immobilise endogenous actin in cytoplasmic lysates isolated from FBS-stimulated human lung fibroblasts treated with PFD at the indicated concentrations followed by actin Western blotting. Bottom panel: Coomassie blue staining of membrane showing His-RPEL fusion proteins used in the pulldown assays. d) Top panel: His-RPEL fusion protein was used to immobilise purified actin in the absence or presence of 1 mM PFD followed by actin Western blotting. Bottom panel: Coomassie blue staining of membrane showing His-RPEL fusion proteins used in the pulldown assays. Data in c) and d) are representative and similar results were seen in three independent experiments. RLU: relative luminescence unit; OD: optical density. p-value calculated using one-way ANOVA. **: p<0.01; ****: p<0.01; NS: not significant.

of cell extracts, in the presence or absence of 1 mM PFD. The result showed that PFD does not enhance the interaction between RPEL and actin in this reconstituted system even at the concentration of 1 mM (figure 6d). Collectively, these data suggest that PFD is likely to promote MRTF–actin physical interaction in an indirect manner, which may serve as the molecular basis of PFD's antagonistic action on MRTF signalling.

PFD attenuates MRTF nuclear localisation in fibroblast foci of IPF lungs

While our data establish PFD as an MRTF inhibitor *in vitro*, the evidence to support MRTF signalling as a clinically achievable target for PFD in human IPF patients is lacking. To this end, we analysed the subcellular localisation of MRTFA in the fibroblast foci regions found in a cohort comprising IPF patients treated with or without PFD or NTD [37]. Quantification of MRTFA immunoreactivity demonstrated that the nuclear MRTFA signal in fibroblast foci is significantly lower in IPF patients treated with PFD than that in IPF patients not treated with PFD (figure 7a and b). Conversely, we observed that the cytoplasmic MRTFA signal in fibroblast foci is significantly higher in IPF patients treated with PFD than that in IPF patients not treated with PFD (figure 7a and b). Additionally, we determined the subcellular localisation of MRTFA in fibroblast foci in IPF patients treated with NTD from the same cohort and found no significant change when compared with untreated IPF patients (figure 7a and b). In support of this observation, we

FIGURE 7 Pirfenidone (PFD) inhibits myocardin-related transcription factor (MRTF) activation in human idiopathic pulmonary fibrosis (IPF) lungs. a) Representative images of MRTFA immunofluorescence signal in fibroblast foci (FF) regions of naïve and PFD- or nintedanib (NTD)-treated IPF lung sections. Scale bar: 20 µm. Arrowhead: nuclear MRTFA in ACTA2^{+} myofibroblasts. b) Nuclear/cytoplasmic distribution of MRTFA in ACTA2^{+} myofibroblasts accumulated within FF regions (n=8 for IPF, n=9 for PFD-treated and n=8 for NTD-treated; certain samples are excluded due to the lack of FF). c) Schematic summary of the proposed mechanism of PFD's inhibitory activity on the MRTF pathway. Data represent mean±SD. DAPI: 4′,6-diamidino-2-phenylindole; ACTA2: α-smooth muscle actin; SRF: serum response factor. p-value calculated using one-way ANOVA. **: $p < 0.01$; NS: not significant.

did not find any impact of NTD (1 µM) on MRTF target gene expression in lung fibroblasts *in vitro* either (supplementary figure S6). On the other hand, we also noticed that neither PFD nor NTD affects MRTFA nuclear/cytoplasmic distribution in EPCAM$^+$ epithelial cells in IPF lungs (supplementary figure S7), supporting the notion that PFD may specifically antagonise MRTF activation in lung fibroblasts and myofibroblasts. In sum, these data suggest that PFD, but not NTD, inhibits *in situ* MRTF activation in human IPF lungs.

Discussion

Within the past few decades, the biomedical community has cured tissue fibrosis many times in animals. However, only PFD, as well as NTD, exhibits clinical benefits in IPF patients [9, 10]. Thus, it is of utmost importance to understand how these medications work to benefit IPF patients. Herein, we, for the first time, establish MRTF signalling as a clinically relevant and achievable target for PFD. This finding is supported by a series of quantitative analyses of PFD's inhibitory effects on MRTF signalling both *in vitro* and *in situ*. In an *in vitro* fibroblast culture system, we measured the inhibitory potency of PFD on MRTF signalling using two complementary readouts: MRTFA nuclear accumulation and MRTF target gene expression. The data from these independent experiments consistently indicate that the IC$_{50}$ of PFD against MRTF signalling ranges between 50 and 150 µM and the maximal inhibition is >90%. To the best of our knowledge, this is the first potency profile of PFD to be reported. More importantly, we presented the human data that PFD attenuates MRTF signalling by ~30% in IPF lungs. Considering that the clinically achievable concentration for PFD is <100 µM in patients [56–58], we propose that PFD is a clinically relevant inhibitor of MRTF signalling in patients.

The molecular basis of PFD's antagonistic action on MRTF signalling was also investigated in the current study. As the main biological activity of PFD is to inhibit MRTF nuclear accumulation, we thoroughly explored whether PFD may modulate the upstream cellular events of this process. To our surprise, we found that PFD appears to promote the interaction between MRTF and actin indirectly without impacting RhoA activation and actin polymerisation. Then, what could be the direct molecular targets of PFD? In this regard, because actin is embedded in a complex cytoskeleton network, it is logical to speculate that PFD may target certain molecular interface(s)/conduit(s) within the cytoskeleton network to modulate MRTF–actin interaction indirectly (figure 7c). This possibility may also help explain the selective effect of PFD on MRTF activation in fibroblasts as the cytoskeleton, a central determinant of cell shape and morphology, is the only subcellular structure that distinguishes fibroblasts from the other cell types [61, 62]. Nonetheless, additional studies are needed to fully delineate the direct action site(s) of PFD within the actin/cytoskeleton network in fibroblasts.

The anti-fibrotic action of PFD has often been linked to its anti-inflammatory and anti-fibrotic activities against pathways such as transforming growth factor-β, tumour necrosis factor-α and p38 signalling [14, 63–65]. However, the main caveat in most studies is the use of excessive and clinically unachievable concentrations (mostly at the millimolar concentration range) of PFD to demonstrate its activity against these pathways. From a pharmacological point of view, the antagonistic activity of PFD on these pathways may be clinically irrelevant and may not contribute to PFD's therapeutic efficacy in patients. In support of this notion, recent studies reported that transforming growth factor-β signalling was not affected by PFD in patient samples [15, 37]. Thus, it is in this context that our finding that establishes PFD as an MRTF inhibitor at clinically achievable concentrations bridges the gap of PFD's pharmacological activity between bench and bedside. On the other hand, since MRTF signalling is a critical regulator of mechano-transduction [22, 28, 29] and the emerging evidence suggests mechanical stress as a key driver of lung fibrosis progression [66, 67], it is possible that PFD's antagonistic action on MRTF signalling might contribute to its therapeutic efficacy.

The major adverse events of PFD in patients include rash, gastrointestinal events, decrease in body weight and elevation of the level of alanine or aspartate aminotransferase in liver [9, 68]. However, MRTF deficiency in both human and mouse has not been reported to be linked to these safety liabilities [23, 69, 70]. One explanation for this discrepancy is that mechanisms underlying PFD's side-effects may be independent from its anti-fibrotic activity. Given the chemical nature of small molecules, it is plausible that PFD could modulate targets other than MRTF signalling to exert its adverse effects in patients. Future studies are therefore warranted to explore non-MRTF targets for PFD, which may enable potential modifications of PFD to improve its therapeutic index in patients.

Up to 45% of deaths in the developed world can be attributed to progressive fibrotic diseases [5]. However, until recently, the development of safe and efficacious anti-fibrotic therapies has been confounded by our poor understanding of the molecular drivers of fibrosis progression in patients. Thus,

our current study that establishes PFD as a clinically relevant MRTF inhibitor may not only shed light on the puzzling anti-fibrotic mechanism of PFD but also illuminate MRTF signalling as a druggable driver of chronic fibrosis progression.

References

1   Kim DS, Collard HR, King TE Jr. Classification and natural history of the idiopathic interstitial pneumonias. *Proc Am Thorac Soc* 2006; 3: 285–292.

2   Flaherty KR, Toews GB, Travis WD, *et al.* Clinical significance of histological classification of idiopathic interstitial pneumonia. *Eur Respir J* 2002; 19: 275–283.

3   King TE Jr, Schwarz MI, Brown K, *et al.* Idiopathic pulmonary fibrosis: relationship between histopathologic features and mortality. *Am J Respir Crit Care Med* 2001; 164: 1025–1032.

4   Nicholson AG, Colby TV, du Bois RM, *et al.* The prognostic significance of the histologic pattern of interstitial pneumonia in patients presenting with the clinical entity of cryptogenic fibrosing alveolitis. *Am J Respir Crit Care Med* 2000; 162: 2213–2217.

5   Wynn TA, Ramalingam TR. Mechanisms of fibrosis: therapeutic translation for fibrotic disease. *Nat Med* 2012; 18: 1028–1040.

6   Coward WR, Saini G, Jenkins G. The pathogenesis of idiopathic pulmonary fibrosis. *Ther Adv Respir Dis* 2010; 4: 367–388.

7   Raghu G, Chen SY, Yeh WS, *et al.* Idiopathic pulmonary fibrosis in US Medicare beneficiaries aged 65 years and older: incidence, prevalence, and survival, 2001–11. *Lancet Respir Med* 2014; 2: 566–572.

8   Collard HR, Chen SY, Yeh WS, *et al.* Health care utilization and costs of idiopathic pulmonary fibrosis in U.S. Medicare beneficiaries aged 65 years and older. *Ann Am Thorac Soc* 2015; 12: 981–987.

9   King TE Jr, Bradford WZ, Castro-Bernardini S, *et al.* A phase 3 trial of pirfenidone in patients with idiopathic pulmonary fibrosis. *N Engl J Med* 2014; 370: 2083–2092.

10   Richeldi L, du Bois RM, Raghu G, *et al.* Efficacy and safety of nintedanib in idiopathic pulmonary fibrosis. *N Engl J Med* 2014; 370: 2071–2082.

11   Hilberg F, Roth GJ, Krssak M, *et al.* BIBF 1120: triple angiokinase inhibitor with sustained receptor blockade and good antitumor efficacy. *Cancer Res* 2008; 68: 4774–4782.

12   Wollin L, Wex E, Pautsch A, *et al.* Mode of action of nintedanib in the treatment of idiopathic pulmonary fibrosis. *Eur Respir J* 2015; 45: 1434–1445.

13   Macias-Barragan J, Sandoval-Rodriguez A, Navarro-Partida J, *et al.* The multifaceted role of pirfenidone and its novel targets. *Fibrogenesis Tissue Repair* 2010; 3: 16.

14   Conte E, Gili E, Fagone E, *et al.* Effect of pirfenidone on proliferation, TGF-beta-induced myofibroblast differentiation and fibrogenic activity of primary human lung fibroblasts. *Eur J Pharm Sci* 2014; 58: 13–19.

15   Knuppel L, Ishikawa Y, Aichler M, *et al.* A novel antifibrotic mechanism of nintedanib and pirfenidone. inhibition of collagen fibril assembly. *Am J Respir Cell Mol Biol* 2017; 57: 77–90.

16   Didiasova M, Singh R, Wilhelm J, *et al.* Pirfenidone exerts antifibrotic effects through inhibition of GLI transcription factors. *FASEB J* 2017; 31: 1916–1928.

17   Ruwanpura SM, Thomas BJ, Bardin PG. Pirfenidone: molecular mechanisms and potential clinical applications in lung disease. *Am J Respir Cell Mol Biol* 2020; 62: 413–422.

18   Xi Y, Li Y, Xu P, *et al.* The anti-fibrotic drug pirfenidone inhibits liver fibrosis by targeting the small oxidoreductase glutaredoxin-1. *Sci Adv* 2021; 7: eabg9241.

19 Iyer SN, Wild JS, Schiedt MJ, *et al.* Dietary intake of pirfenidone ameliorates bleomycin-induced lung fibrosis in hamsters. *J Lab Clin Med* 1995; 125: 779–785.

20 Raghu G, Johnson WC, Lockhart D, *et al.* Treatment of idiopathic pulmonary fibrosis with a new antifibrotic agent, pirfenidone: results of a prospective, open-label phase II study. *Am J Respir Crit Care Med* 1999; 159: 1061–1069.

21 Miano JM, Long X, Fujiwara K. Serum response factor: master regulator of the actin cytoskeleton and contractile apparatus. *Am J Physiol Cell Physiol* 2007; 292: C70–C81.

22 Olson EN, Nordheim A. Linking actin dynamics and gene transcription to drive cellular motile functions. *Nat Rev Mol Cell Biol* 2010; 11: 353–365.

23 Record J, Malinova D, Zenner HL, *et al.* Immunodeficiency and severe susceptibility to bacterial infection associated with a loss-of-function homozygous mutation of MKL1. *Blood* 2015; 126: 1527–1535.

24 Esnault C, Stewart A, Gualdrini F, *et al.* Rho-actin signaling to the MRTF coactivators dominates the immediate transcriptional response to serum in fibroblasts. *Genes Dev* 2014; 28: 943–958.

25 Tschumperlin DJ, Ligresti G, Hilscher MB, *et al.* Mechanosensing and fibrosis. *J Clin Invest* 2018; 128: 74–84.

26 Lighthouse JK, Small EM. Transcriptional control of cardiac fibroblast plasticity. *J Mol Cell Cardiol* 2016; 91: 52–60.

27 Miralles F, Posern G, Zaromytidou AI, *et al.* Actin dynamics control SRF activity by regulation of its coactivator MAL. *Cell* 2003; 113: 329–342.

28 Gau D, Roy P. SRF'ing and SAP'ing – the role of MRTF proteins in cell migration. *J Cell Sci* 2018; 131: jcs218222.

29 Small EM. The actin–MRTF–SRF gene regulatory axis and myofibroblast differentiation. *J Cardiovasc Transl Res* 2012; 5: 794–804.

30 Li Z, Chen B, Dong W, *et al.* MKL1 promotes endothelial-to-mesenchymal transition and liver fibrosis by activating TWIST1 transcription. *Cell Death Dis* 2019; 10: 899.

31 Mao L, Liu L, Zhang T, *et al.* MKL1 mediates TGF-beta-induced CTGF transcription to promote renal fibrosis. *J Cell Physiol* 2020; 235: 4790–4803.

32 Shiwen X, Stratton R, Nikitorowicz-Buniak J, *et al.* A role of myocardin related transcription factor-A (MRTF-A) in scleroderma related fibrosis. *PLoS One* 2015; 10: e0126015.

33 Yu-Wai-Man C, Treisman R, Bailly M, *et al.* The role of the MRTF-A/SRF pathway in ocular fibrosis. *Invest Ophthalmol Vis Sci* 2014; 55: 4560–4567.

34 Bernau K, Ngam C, Torr EE, *et al.* Megakaryoblastic leukemia-1 is required for the development of bleomycin-induced pulmonary fibrosis. *Respir Res* 2015; 16: 45.

35 Small EM, Thatcher JE, Sutherland LB, *et al.* Myocardin-related transcription factor-A controls myofibroblast activation and fibrosis in response to myocardial infarction. *Circ Res* 2010; 107: 294–304.

36 Fan Z, Hao C, Li M, *et al.* MKL1 is an epigenetic modulator of TGF-beta induced fibrogenesis. *Biochim Biophys Acta* 2015; 1849: 1219–1228.

37 Zhang Y, Jones KD, Achtar-Zadeh N, *et al.* Histopathological and molecular analysis of idiopathic pulmonary fibrosis lungs from patients treated with pirfenidone or nintedanib. *Histopathology* 2019; 74: 341–349.

38 Ware LB, Wang Y, Fang X, *et al.* Assessment of lungs rejected for transplantation and implications for donor selection. *Lancet* 2002; 360: 619–620.

39 Pau GRJ. HTSeqGenie: a NGS analysis pipeline. 2013. https://bioconductor.org/packages/release/bioc/manuals/HTSeqGenie/man/HTSeqGenie.pdf Date last accessed: 3 January 2023.

40 Srinivasan K, Friedman BA, Larson JL, *et al.* Untangling the brain's neuroinflammatory and neurodegenerative transcriptional responses. *Nat Commun* 2016; 7: 11295.

41 Law CW, Chen Y, Shi W, *et al.* voom: precision weights unlock linear model analysis tools for RNAseq read counts. *Genome Biol* 2014; 15: R29.

42 Wu D, Smyth GK. Camera: a competitive gene set test accounting for inter-gene correlation. *Nucleic Acids Res* 2012; 40: e133.

43 Subramanian A, Tamayo P, Mootha VK, *et al.* Gene set enrichment analysis: a knowledge-based approach for interpreting genome-wide expression profiles. *Proc Natl Acad Sci USA* 2005; 102: 15545–15550.

44 R Core Team. R: A Language and Environment for Statistical Computing. Vienna, R Foundation for Statistical Computing, 2018.

45 Ding N, Zhou H, Esteve PO, *et al.* Mediator links epigenetic silencing of neuronal gene expression with X-linked mental retardation. *Mol Cell* 2008; 31: 347–359.

46 DePianto DJ, Heiden JAV, Morshead KB, *et al.* Molecular mapping of interstitial lung disease reveals a phenotypically distinct senescent basal epithelial cell population. *JCI Insight* 2021; 6: e143626.

47 Selman M, Carrillo G, Estrada A, *et al.* Accelerated variant of idiopathic pulmonary fibrosis: clinical behavior and gene expression pattern. *PLoS One* 2007; 2: e482.

48 Yang IV, Coldren CD, Leach SM, *et al.* Expression of cilium-associated genes defines novel molecular subtypes of idiopathic pulmonary fibrosis. *Thorax* 2013; 68: 1114–1121.

49   Ahluwalia N, Grasberger PE, Mugo BM, *et al.* Fibrogenic lung injury induces non-cell-autonomous fibroblast invasion. *Am J Respir Cell Mol Biol* 2016; 54: 831–842.

50   Tager AM, LaCamera P, Shea BS, *et al.* The lysophosphatidic acid receptor LPA1 links pulmonary fibrosis to lung injury by mediating fibroblast recruitment and vascular leak. *Nat Med* 2008; 14: 45–54.

51   Geng Y, Liu X, Liang J, *et al.* PD-L1 on invasive fibroblasts drives fibrosis in a humanized model of idiopathic pulmonary fibrosis. *JCI Insight* 2019; 4: e125326.

52   Li Y, Jiang D, Liang J, *et al.* Severe lung fibrosis requires an invasive fibroblast phenotype regulated by hyaluronan and CD44. *J Exp Med* 2011; 208: 1459–1471.

53   Xie X, Lu J, Kulbokas EJ, *et al.* Systematic discovery of regulatory motifs in human promoters and 3′ UTRs by comparison of several mammals. *Nature* 2005; 434: 338–345.

54   Sivakumar P, Thompson JR, Ammar R, *et al.* RNA sequencing of transplant-stage idiopathic pulmonary fibrosis lung reveals unique pathway regulation. *ERJ Open Res* 2019; 5: 00117-2019.

55   Xi Y, LaCanna R, Ma HY, *et al.* A WISP1 antibody inhibits MRTF signaling to prevent the progression of established liver fibrosis. *Cell Metab* 2022; 34: 1377–1393.

56   Wollin L, Schuett J, Ostermann A. The effect of nintedanib compared to pirfenidone on serum-stimulated proliferation of human primary lung fibroblasts at clinically relevant concentrations. *Am J Respir Crit Care Med* 2015; 191: A4940.

57   Shi S, Wu J, Chen H, *et al.* Single- and multiple-dose pharmacokinetics of pirfenidone, an antifibrotic agent, in healthy Chinese volunteers. *J Clin Pharmacol* 2007; 47: 1268–1276.

58   Rubino CM, Bhavnani SM, Ambrose PG, *et al.* Effect of food and antacids on the pharmacokinetics of pirfenidone in older healthy adults. *Pulm Pharmacol Ther* 2009; 22: 279–285.

59   Treisman R. Ternary complex factors: growth factor regulated transcriptional activators. *Curr Opin Genet Dev* 1994; 4: 96–101.

60   Yu FX, Zhao B, Panupinthu N, *et al.* Regulation of the Hippo-YAP pathway by G-protein-coupled receptor signaling. *Cell* 2012; 150: 780–791.

61   Tarin D, Croft CB. Ultrastructural features of wound healing in mouse skin. *J Anat* 1969; 105: 189–190.

62   Kalluri R, Zeisberg M. Fibroblasts in cancer. *Nat Rev Cancer* 2006; 6: 392–401.

63   Schaefer CJ, Ruhrmund DW, Pan L, *et al.* Antifibrotic activities of pirfenidone in animal models. *Eur Respir Rev* 2011; 20: 85–97.

64   Oku H, Nakazato H, Horikawa T, *et al.* Pirfenidone suppresses tumor necrosis factor-alpha, enhances interleukin-10 and protects mice from endotoxic shock. *Eur J Pharmacol* 2002; 446: 167–176.

65   Nakazato H, Oku H, Yamane S, *et al.* A novel anti-fibrotic agent pirfenidone suppresses tumor necrosis factor-alpha at the translational level. *Eur J Pharmacol* 2002; 446: 177–185.

66   Wu H, Yu Y, Huang H, *et al.* Progressive pulmonary fibrosis is caused by elevated mechanical tension on alveolar stem cells. *Cell* 2020; 180: 107–121.

67   Herrera J, Henke CA, Bitterman PB. Extracellular matrix as a driver of progressive fibrosis. *J Clin Invest* 2018; 128: 45–53.

68   Noble PW, Albera C, Bradford WZ, *et al.* Pirfenidone in patients with idiopathic pulmonary fibrosis (CAPACITY): two randomised trials. *Lancet* 2011; 377: 1760–1769.

69   Sun Y, Boyd K, Xu W, *et al.* Acute myeloid leukemia-associated *Mkl1* (*Mrtf-a*) is a key regulator of mammary gland function. *Mol Cell Biol* 2006; 26: 5809–5826.

70   Li S, Chang S, Qi X, *et al.* Requirement of a myocardin-related transcription factor for development of mammary myoepithelial cells. *Mol Cell Biol* 2006; 26: 5797–5808.